ISIJ International, Vol. 62 (2022), No. 1, pp. 263–274
https://doi.org/10.2355/isijinternational.ISIJINT-2021-121

Kinetics of Calcium Leaching from Particulate Steelmaking Slag in Acetic Acid Solution

Eishi KUSAKA,[1)]* Ryoma SUEHIRO[1)] and Yoshiharu IWAMIZU[2)]

1) Graduate School of Energy Science, Kyoto University, Sakyo-ku, Kyoto, 606-8501 Japan.
2) Kure Area, Setouchi Works, Nippon Steel Co., 11-1 Showa-cho, Kure, Hiroshima, 737-8520 Japan.

(*Received on March 25, 2021; accepted on September 7, 2021*)

In order to reduce CO_2 emission, the CO_2 sequestration using particulate steelmaking slag in water is world widely being studied through a Ca-carbonation method. As consequence, the improved efficiency of Ca leaching from the steelmaking-slag particles contributes significantly to increasing the amount of fixed CO_2. Therefore, in this study, for the purpose of understanding the Ca leaching from steelmaking slag particles, the rate of Ca leaching in week acidic solution was analyzed by several leaching kinetics models such as the shrinking core model and the logarithmic rate law. In addition to Ca, the leaching rate of Fe which is one of the major elements was also investigated. The Ca and Fe leaching process with stirring could be fitted well by logarithmic rate law. Moreover, by the observation using SEM-EDX, it was observed that the residue after acetic acid leaching was porous material with the pores blocked. From these results, it was revealed that the mass transfer in the products blocking the pore surface of slag particles was very likely to be the rate-controlling step of Ca leaching. In fact, promoting mass transfer by ultrasonic irradiation could enhance the rate of Ca leaching remarkably. While the Ca leaching ratio reaches 56.6% at 300 min without ultrasonic irradiation, the leaching ratio reaches 57.3% just for 30 min leaching with ultrasonic irradiation. This study reveals that promoting the mass transfer in the products blocking the pore surface of slag particles is important for increasing the rate of Ca leaching.

KEY WORDS: steelmaking slag; kinetics analysis; leaching; mass transfer; CO_2 sequestration.

1. Introduction

Since carbon dioxide (CO_2) is known as the greenhouse gas which mainly causes global warming, reduction of CO_2 emission is considered to be necessary. Therefore, the technology of mineral carbonation attracts much attention for CO_2 sequestration. The fundamental concept of mineral carbonation is to imitate natural weathering processes in which the minerals containing Ca/Mg silicates are converted into their carbonates:[1)]

$$(Ca,Mg)SiO_3(s) + CO_2(g) \rightleftharpoons (Ca,Mg)CO_3(s) + SiO_2(s) \quad \text{..... (1)}$$

In addition, the aqueous mineral carbonation of Ca/Mg silicates can be written as bellow:[1)]

$$CO_2(g) + H_2O(l) \rightleftharpoons 2H^+(aq) + CO_3^{2-}(aq) \quad \text{..... (2)}$$

$$(Ca,Mg)SiO_3(s) + 2H^+(aq) \rightleftharpoons (Ca,Mg)^{2+}(aq) + SiO_2(s) + H_2O(l) \quad \text{..... (3)}$$

$$(Ca,Mg)^{2+}(aq) + CO_3^{2-}(aq) \rightleftharpoons (Ca,Mg)CO_3 \downarrow (s) \quad \text{.... (4)}$$

In case of Ca/Mg oxide, Eqs. (1) and (3) are written respectively as follows:

$$(Ca,Mg)O(s) + CO_2(g) \rightleftharpoons (Ca,Mg)CO_3(s) \quad \text{..... (1)'}$$

$$(Ca,Mg)O(s) + 2H^+(aq) \rightleftharpoons (Ca,Mg)^{2+}(aq) + H_2O(l) \quad \text{..... (3)'}$$

The CO_2 which reacted with Ca or Mg can be stored for a long time due to the thermodynamic stability of the carbonate products. Moreover, the cost of energy input might be able to be reduced since the overall carbonation reaction is exothermic reaction.[2)] However, in fact, as the energy input is necessary for the preparation and processing of the solid reactants, the mineral carbonation is expensive process.[3)] Therefore, it is almost impossible to use the natural and rare silicate minerals containing Ca such as wollastonite for mineral carbonation.[4)] Thus, the mineral carbonation processes which utilize industrial wastes such as coal fly ash,[5,6)] cement kiln dust[7)] and slag[8–10)] have been studied. These industrial wastes are suitable for the raw materials of mineral

* Corresponding author: E-mail: kusaka@energy.kyoto-u.ac.jp

carbonation because the Ca-oxide content is high and these wastes are low cost as mining is not needed. In this study, we focused on steelmaking slag for the raw materials of mineral carbonation. Steelmaking slag is byproduct from the steel making process and about 14 Mt of steelmaking slag are produced annually in Japan.[11] Although there are several issues about using untreated steelmaking slag in civil engineering such as volume expansion and the leaching of heavy metal, Pan *et al.* have indicated the probability that these issues could be overcome by the deployment of accelerated carbonation.[12] Moreover, in Japan, the CO_2 emission of steel industry in 2018 reached 158 Mt, which accounted for about 14% of overall CO_2 emission.[13,14] Therefore, the CO_2 sequestration using steelmaking slag is significant for reduction of a large amount of CO_2 emission in steel industry.

Hujigen *et al.*[1] have studied the aqueous mineral carbonation with steelmaking slag and found that the carbonation reaction occurs in two steps. The first step is Ca leaching from steelmaking slag particles into the solution (Eq. (3)) and the second step is precipitation of calcite on the surface of the particles (Eq. (4)). In addition, they also reported that the Ca leaching was rate-controlling step of the carbonation process. Therefore, increasing the rate of Ca leaching from the steelmaking slag will contribute to increasing the amount of fixed CO_2. Hence, it is important to understand the Ca leaching mechanism from steelmaking slag in order to realize the efficient carbonation process.

There are many studies about discussing the dissolution mechanism of Ca from steelmaking slag in iron and steel field.[15–18] Zhang *et al.*[15] investigated the dissolution behavior from steelmaking slag into seawater and found that the more Ca of slag with large CaO/SiO_2 ratio dissolved than that with small ratio. Zhu *et al.*[16] reported that the amount of α-$CaO{\cdot}SiO_2$, β-$CaO{\cdot}SiO_2$, $3CaO{\cdot}2SiO_2$, $2CaO{\cdot}MgO{\cdot}2SiO_2$ and $3CaO{\cdot}MgO{\cdot}2SiO_2$ in steelmaking slag should be restrained to suppress the Ca elution. In addition, several researchers carried out the kinetics analysis of Ca leaching from slag into water using kinetics models in order to clarify the leaching mechanism precisely.[17,18] Yokoyama *et al.*[17] showed that the leaching of Ca from the slag was controlled by the diffusion through the surface layer, and Kashiwaya *et al.*[18] reported that the rate-controlling step of Ca leaching changed when the particle size increased. However, these investigations on the kinetics did not carried out in the aqueous conditions where Ca-precipitation is difficult to occur. Therefore, the analysis of the rate of Ca leaching from particulate steelmaking slag in acidic solution seems to be important, because it is assumed that the leaching mechanism in weak acidic pH is different from that in neutral to alkaline solution where Ca is easily precipitated. Although several researchers recently investigated the Ca leaching behavior from steelmaking slag in acidic solution,[19,20] there are few studies focusing on the kinetics analysis of Ca leaching in acidic condition. It seems to be further important to understand the first step of diffusion to the aqueous phase of Ca^{2+} that reacts with carbonate ion (CO_3^{2-}).

In other fields in addition to iron and steel industry, several researchers have ever studied the Ca leaching from slag with acid solution for the purpose of CO_2 sequestration.[21–25] They have investigated the effects of several parameters such as particle size, solution temperature, acid concentration and solid to liquid ratio for Ca leaching ratio. As a result, it was revealed that the Ca leaching ratio increased as the particle size or solid to liquid ratio decreased or acid concentration increased. However, they did not carry out kinetics analysis of Ca leaching from slag.

From the above, in this study, we analyzed the rate of Ca leaching in weak acidic condition using acetic acid by several leaching kinetics models for the purpose of understanding the Ca leaching as well as the first step of diffusion of Ca^{2+} to the aqueous phase from particulate steelmaking slag. Acetic acid is thought to be appropriate for the kinetics analysis of Ca leaching as acetate ion does not form poor soluble products with Ca ion. In addition to Ca, we also investigated the leaching rate of Fe which is one of the major elements composing of steelmaking slag.

2. Experimental

2.1. Material

The sample used in this study was the steelmaking slag provided by a steel manufacture in Japan and the sample was sieved to a grain size of 0.50–1.0 mm. The contents of Ca and Fe were measured by using inductively coupled plasma-optical emission spectrometry (Thermo Fisher Scientific, iCAP™ 7000 ICP-OES) after Ca and Fe in the sample were dissolved completely with aqua regia. The contents of Ca and Fe in the steelmaking slag sample are 36.6 wt% and 19.5 wt%, respectively. Furthermore, the mineral phases of the slag sample were investigated using XRD (Shimadzu Corporation, XRD-6000). **Figure 1** shows the XRD spectra of the sample. The untreated slag sample includes larnite (Ca_2SiO_4), wüstite (FeO), brownmillerite ($Ca_2(Al,Fe)_2O_5$), merwinite ($Ca_3Mg(SiO_4)_2$), srebrodolskite ($Ca_2Fe_2O_5$) and portlandite ($Ca(OH)_2$). In fact, these mineral phases have already been reported by many researchers.[24,26,27]

2.2. Procedure

The Ca and Fe leaching experiments were carried out in a 1.5 L separable flask at the solution temperature of 281 K, 293 K (room temperature), or 333 K. The temperature was controlled by a temperature-controlled water bath. The acetic acid solution of 1 L was put into the flask and the solution was stirred at 0 to 300 rpm by using a mechanical stirrer. When the solution temperature became stable, 1.0 g of the slag sample was added to the flask. After a predetermined period of time, 2 ml samples were taken from the solution and then the solution samples were immediately filtered using a membrane filter of 0.8 μm pore size. Afterwards, the concentration of Ca and Fe in the samples were measured by using ICP-OES. Nitrogen gas was bubbled through the separable flask at 200 ml/min during the leaching experiments in order to prevent carbon dioxide in air from dissolving in the solution.

The Ca and Fe leaching ratio were defined as the below equation:

$$\text{Ca(Fe) leaching ratio}[\%] = \frac{\text{Ca(Fe) leaching quantity from slag sample}\,[\text{mol}]}{\text{Ca(Fe) content in slag sample dissolved in aqua regia}\,[\text{mol}]} \times 100 \quad \text{..... (5)}$$

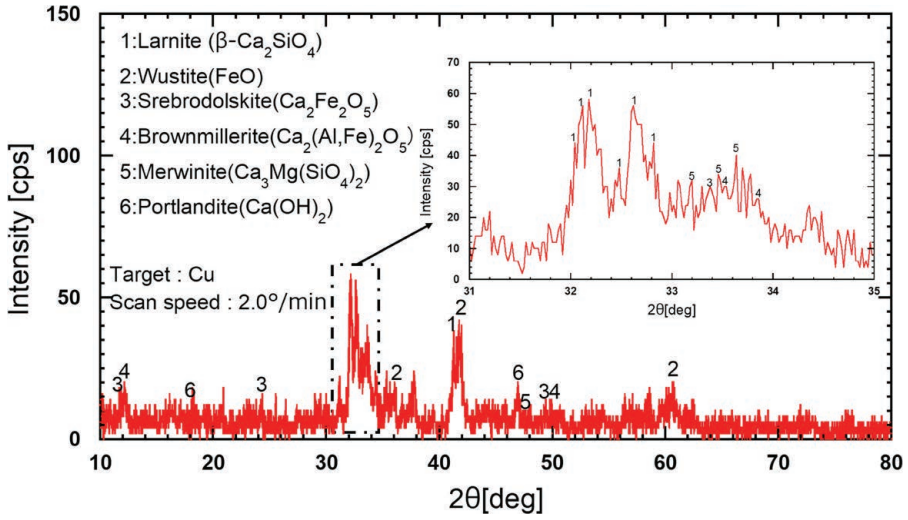

Fig. 1. XRD spectra of the untreated slag. (Online version in color.)

3. Results and Discussion

3.1. Effect of Acetic Acid Concentration

Figure 2 shows the effect of acetic acid concentration on the leaching of Ca from the steelmaking slag in the solutions containing 0, 0.04, and 0.28 mol/L of acetic acid. As can be seen in Fig. 2, the Ca leaching rate increases as the acetic acid concentration increases. At the leaching time of 300 min, the ratio reaches 7.2%, 44.7%, and 56.6% at the concentration of 0, 0.04, and 0.28 mol/L, respectively. In addition, the pH's before and after leaching are shown in **Table 1**, which indicates that pH decreases as the acetic acid concentration increases. With the acetic acid concentration increasing, more acetic acid molecules can participate in the reaction of Ca dissolution. Therefore, increasing the acetic acid concentration can promote the Ca leaching rate. Subsequent experiments were carried out at the acetic acid concentration of 0.28 mol/L in order to keep the pH around 3.

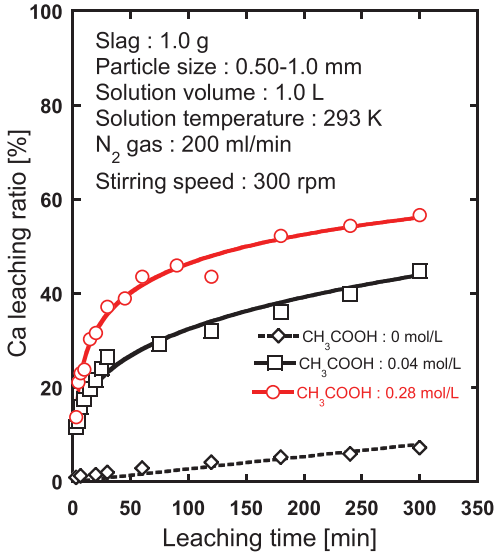

Fig. 2. Effect of acetic acid concentration for Ca leaching. (Online version in color.)

Table 1. The difference of pH before and after leaching.

Acetic acid concentration (mol/L)	pH	
	Before leaching	After leaching
0.0	–	9.84
0.04	2.83	3.90
0.28	2.39	3.14

3.2. Effect of Stirring Speed

The effect of stirring speed on the leaching of Ca and Fe from the steelmaking slag was investigated at the stirring speed of 0, 100, and 300 rpm at the solution temperature of 293 K. **Figures 3**(a) and 3(b) show the change in Ca and Fe leaching rate with varying the leaching time, respectively. As can be seen in Fig. 3(a), stirring speed has a remarkable effect for increasing the Ca leaching rate up to 100 rpm. Although the maximum Ca leaching ratio is 26.9% without stirring, the ratio increases up to 52.9% at 100 rpm. However, the leaching rate increases slightly when the stirring speed increases from 100 to 300 rpm. Figure 3(b) also indicates that the Fe leaching rate is greatly affected by stirring speed up to 100 rpm and is slightly affected from 100 to 300 rpm. The Fe leaching ratio increases linearly without stirring and reaches 8.2% at 300 min. With the stirring speed increasing from 100 to 300 rpm, the ratio increases from 15.9% to 20.1% after 300 min.

When the rate of dissolution increases as the stirring speed increases in a solid-liquid reaction, this process is the one diffusion-controlled. Since the thickness of liquid film decreases with increasing stirring speed, the rate of dissolution also increases.[28] Therefore, at 300 rpm, the mass transfer in liquid film can be negligible on the leaching of Ca and Fe. All subsequent experiments were carried out at 300 rpm in order to disregard the effect of mass transfer in liquid film.

3.3. Effect of Solution Temperature

Since it was revealed that stirring speed affected the Ca and Fe leaching rate from the results in Section 3.2, the Ca and Fe leaching process might be controlled by diffusion in the liquid film. In general, the mass transfer in liquid film can be promoted as the solution temperature increases. Therefore, the solution temperature may affect the Ca and Fe

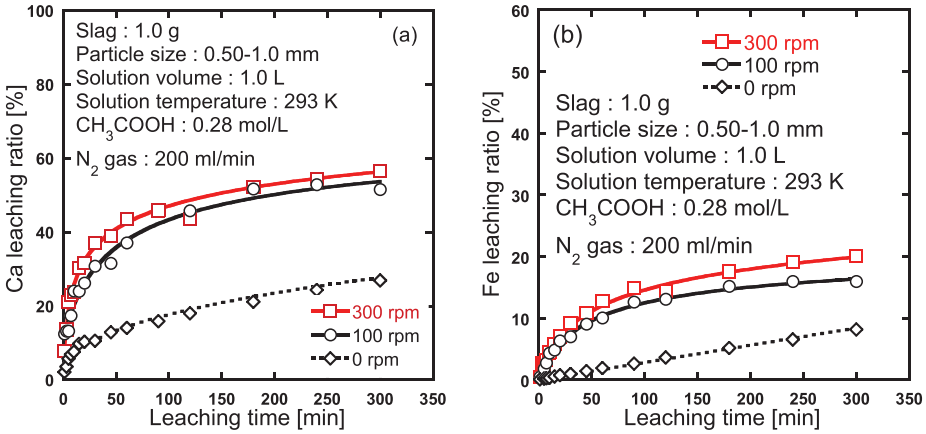

Fig. 3. Effect of stirring speed for Ca leaching (a) and Fe leaching (b). (Online version in color.)

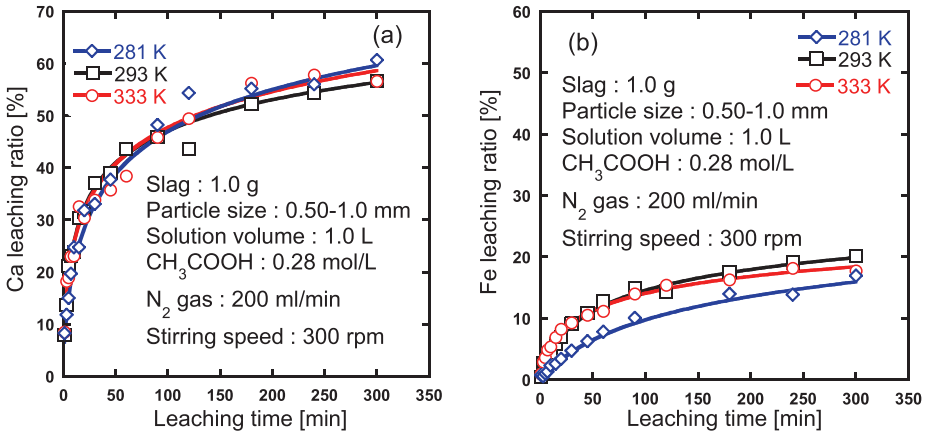

Fig. 4. Effect of solution temperature for Ca leaching (a) and Fe leaching (b). (Online version in color.)

leaching rate. For this reason, the effect of temperature on the leaching of Ca and Fe from the steelmaking slag was investigated at temperatures of 281, 293, and 333 K in this section.

Figures 4(a) and 4(b) show the Ca and Fe leaching curve at the stirring speed of 300 rpm and the acetic acid concentration of 0.28 mol/L. As can be seen in Fig. 4(a), temperature has a small effect on the Ca leaching. Some researchers have investigated the effect of temperature on the Ca leaching from steelmaking slag. Eloneva *et al.*[22] reported that the dissolution of Ca from the steelmaking slag was hardly dependent on the solution temperature in acetic acid. Furthermore, Mattila *et al.*[23] reported that the solution temperature hardly affected the Ca leaching kinetics in an ammonium nitrate solution. Figure 4(b) indicates that Fe leaching behavior at 293 K and 333 K are almost the same, while the leaching rate at 281 K is lower than 293 K and 333 K.

Judging from the results of Figs. 4(a) and 4(b), it was found that the solution temperature affected Fe leaching but did not affect Ca leaching. Although the temperature dependence of Fe leaching rate might be caused by the effect of chemical reaction, further detailed investigations should be needed concerning the Fe leaching since the main object of this study is Ca.

3.4. Kinetics Analysis of Leaching

3.4.1. Leaching Kinetics Model

The Ca and Fe leaching from steelmaking slag is solid-liquid heterogeneous reactions. Shrinking core model (SCM) has been often used for the leaching kinetics analysis of solid-liquid heterogenous reactions. The SCM assumes that reaction occurs first at the outer skin of the particle and then the reaction zone moves into the solid, leaving behind "ash", that is, completely converted material and inert solid.[29] The ash layer formed during the leaching process of steelmaking slag is the insoluble Ca depleted rim which surrounds the unreacted core and has porous structure.[30] Therefore, the Ca ion must pass through the pores of ash layer to the balk aqueous phase for the Ca extraction from steelmaking slag. According to the SCM, there are three types of rate-controlling steps during leaching process: diffusion through the liquid film, the surface chemical reaction and diffusion through the ash layer. The kinetics equations of the SCM expressing each rate-controlling step can be described as bellow.[29]

If the leaching process is controlled by the liquid film diffusion, the kinetics equation can be expressed as

$$R = \mathrm{k}t \quad \cdots\cdots (6)$$

If the leaching process is controlled by the chemical reaction, the kinetics equation can be expressed as

$$1-(1-R)^{\frac{1}{3}} = \mathrm{k}t \quad \cdots\cdots (7)$$

If the leaching process is controlled by ash layer diffusion, the kinetics equation can be expressed as

$$1-3(1-R)^{\frac{2}{3}}+2(1-R) = \mathrm{k}t \quad \cdots\cdots (8)$$

where R is the leaching ratio of elements; k is the apparent

rate constant; t is the leaching time.

When the leaching reaction did not fit the SCM, another leaching kinetics model should be applied to the results of leaching experiments. If the leaching ratio decreases rapidly with the passage of time, the kinetics equation (referred to as "logarithmic rate law") can be expressed as

$$R = \mathrm{k} \log t + \mathrm{C} \quad \text{..... (9)}$$

where R is the leaching ratio of elements; k, C are constants; t is the leaching time.[31] If the rate-controlling step of the leaching reaction is mass transfer in the coating of products due to the formation and disappearance in slits on the coating, the reaction follows the logarithmic rate law.[32]

In this study, logarithmic rate law in addition to the SCM were applied to the leaching of Ca and Fe for understanding the mechanism of Ca leaching from the steelmaking slag.

3.4.2. Kinetics Analysis with Different Stirring Speed

Figures 5(a)–5(d) and **6**(a)–6(d) show the plots of applying Eqs. (6)–(9), respectively, to the leaching behavior of Ca and Fe at different stirring speed. In addition, the determination coefficients (R^2) in Figs. 5 and 6 are listed in **Table 2**.

As can be seen in Figs. 5(a) to 5(d), the Ca leaching curve without stirring can be linearized by using the ash layer diffusion model (Eq. (8)) in the range of 3 to 300 min. The R^2 value is 0.9930 which is the nearest to 1 of the other kinetics models. Therefore, the Ca leaching process without stirring is controlled by ash layer diffusion until 300 min. However, at the stirring speed of 100 rpm and 300 rpm, the Ca leaching process cannot be fitted by the SCM, whereas can be fitted well by logarithmic rate law (Eq. (9)). This is because stirring promotes mass transfer in the ash layer, and thereby the rate-controlling step changes. Because of the good correlation with logarithmic rate law, the Ca leaching process with stirring is presumed to be inhibited by the poorly soluble coating of product covering the particle surface.

Figures 6(a)–6(d) indicates that the Fe leaching curve without stirring can be fitted well with both liquid film diffusion model (Eq. (6)) and surface chemical reaction model (Eq. (7)) in the range of 3 to 300 min. The R^2 value of liquid film diffusion model and surface chemical reaction model is 0.9982 and 0.9986, respectively. Therefore, the Fe leaching process without stirring is controlled by both liquid film diffusion and chemical reaction until 300 min. However, the rate-controlling step of Fe leaching process changes at the stirring speed of 100 and 300 rpm. The Fe leaching process with stirring cannot be linearized by the SCM but can be linearized by logarithmic rate law.

From the above results, the Ca and Fe leaching process with stirring give the best correlation with logarithmic rate law.

3.4.3. Kinetics Analysis with Different Temperature

Figures 7(a)–7(d) and **8**(a)–8(d) show the plots of applying Eqs. (6)–(9), respectively, to the leaching behavior of Ca and Fe at different temperature. The determination coefficients (R^2) in Figs. 7 and 8 are listed in **Table 3**. As can be seen in Figs. 7(a)–7(d), the Ca leaching process until 300 min can be fitted well by logarithmic rate law in

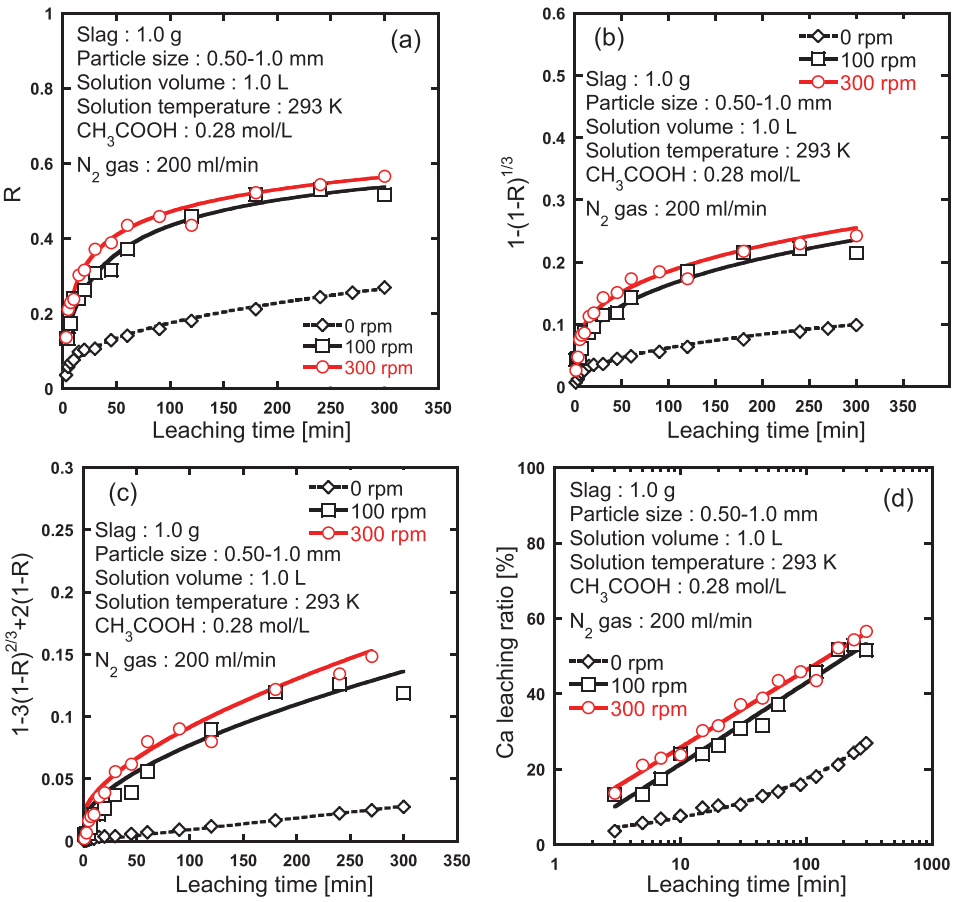

Fig. 5. Leaching kinetics model applied to Ca leaching at different stirring speed (Liquid film diffusion model (a), Surface chemical reaction model (b), Ash layer diffusion model (c), Logarithmic rate law (d)). (Online version in color.)

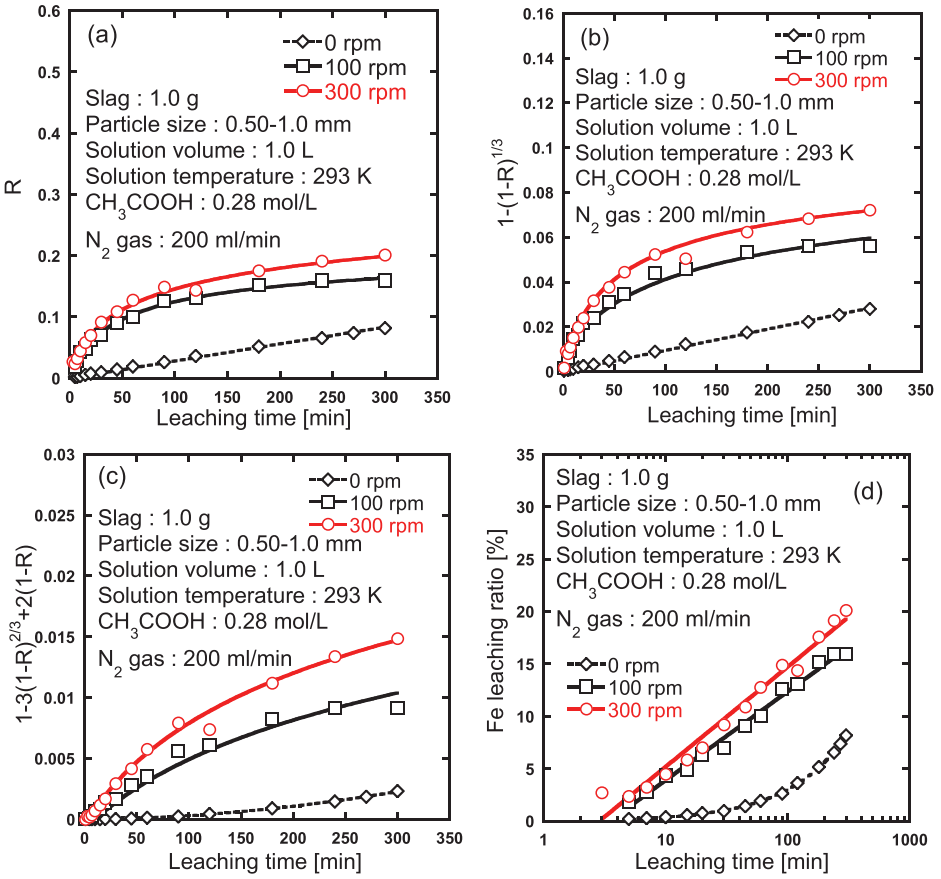

Fig. 6. Leaching kinetics model applied to Fe leaching at different stirring speed (Liquid film diffusion model (a), Surface chemical reaction model (b), Ash layer diffusion model (c), Logarithmic rate law (d)). (Online version in color.)

Table 2. The determination coefficients of various kinetics models at different stirring speed.

Element	Stirring speed [rpm]	Determination coefficients (R^2)			
		$R = kt$	$1-(1-R)^{1/3} = kt$	$1-3(1-R)^{2/3}+2(1-R) = kt$	$R = k \log t + C$
Ca	0	0.8586	0.8746	0.9930	0.9313
	100	0.7384	0.7801	0.9181	0.9763
	300	0.6981	0.7418	0.8924	0.9849
Fe	0	0.9982	0.9986	0.9487	0.7431
	100	0.8252	0.8332	0.9459	0.9897
	300	0.8332	0.8440	0.9659	0.9747

the temperature range of 281–333 K and the R^2 value are respectively 0.9548, 0.9849 and 0.9646 at 281 K, 293 K, and 333 K. Therefore, the rate-controlling step of the Ca leaching process does not change in the range of 281–333 K and is likely to be the mass transfer in the products covering the particle surface. Although the Ca leaching rate was hardly dependent on the solution temperature in the range of 281–333 K from the results in Section 3.3, the leaching rate should decrease with increasing the solution temperature from the point of view of thermodynamics. For instance, since the dissolution reaction of lime (CaO) is exothermic reaction, the leaching rate should decrease by temperature increase. However, in general, increasing the solution temperature also contributes to promoting the diffusion of molecules in aqueous phase. Therefore, it is assumed that the diffusion of Ca^{2+} in the products covering the slag particles is promoted with increasing the solution temperature and thereby the Ca leaching rate hardly decreases even though the solution temperature increases. For this reason, it seems to be very important to promote the diffusion of Ca^{2+} in the products in the slag-particle surface region for increasing the leaching rate.

On the other hand, the solution temperature affects the rate-controlling step of Fe leaching as shown in Figs. 8(a)–8(d). The Fe leaching process can be linearized with ash layer diffusion model at the temperature of 281 K in the range of 3 to 300 min, while give the best correlation with logarithmic rate law at the temperature of 293 K and 333 K. In short, it is found that the appropriate kinetics model for Fe leaching process shifts from ash layer diffusion model to logarithmic rate law as the solution temperature increases.

3.5. Morphology of the Solid Residues

From the kinetics analysis in Section 3.4, the Ca leach-

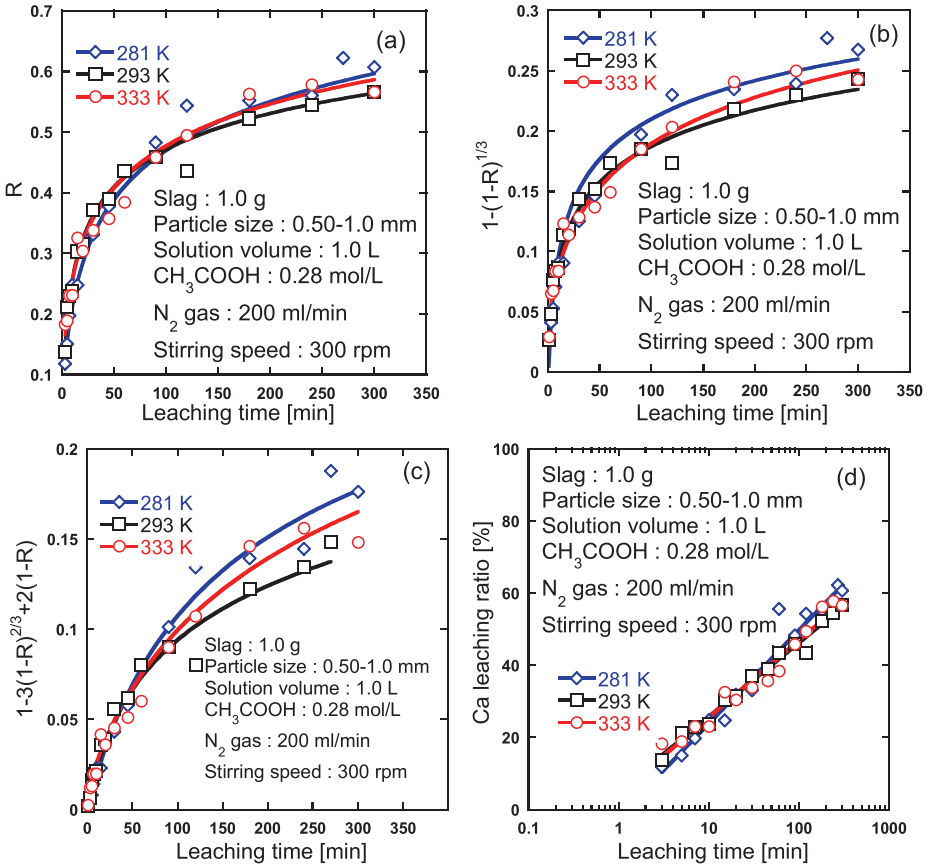

Fig. 7. Leaching kinetics model applied to Ca leaching at different solution temperature (Liquid film diffusion model (a), Surface chemical reaction model (b), Ash layer diffusion model (c), Logarithmic rate law (d)). (Online version in color.)

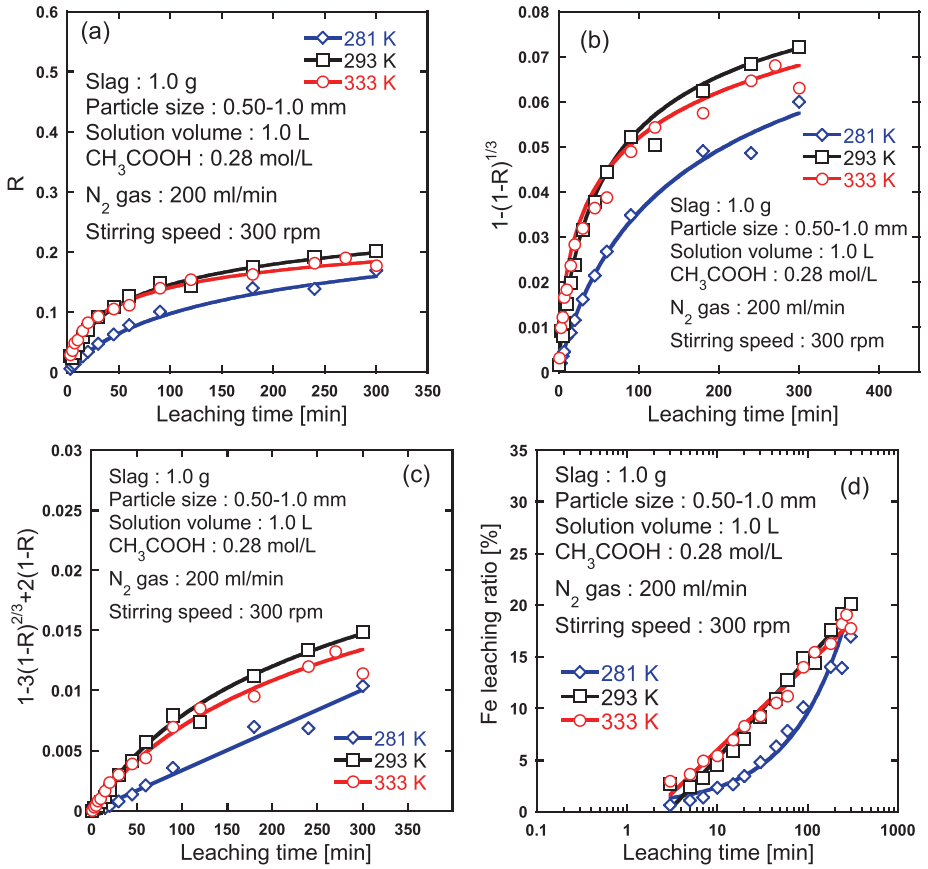

Fig. 8. Leaching kinetics model applied to Fe leaching at different solution temperature (Liquid film diffusion model (a), Surface chemical reaction model (b), Ash layer diffusion model (c), Logarithmic rate law (d)). (Online version in color.)

Table 3. The determination coefficients of various kinetics models at different solution temperature.

Element	Temperature [K]	Determination coefficients (R^2)			
		$R = kt$	$1-(1-R)^{1/3} = kt$	$1-3(1-R)^{2/3}+2(1-R) = kt$	$R = k \log t + C$
Ca	281	0.7548	0.7936	0.8887	0.9548
	293	0.6981	0.7418	0.8924	0.9849
	333	0.7223	0.7697	0.9135	0.9646
Fe	281	0.9152	0.9221	0.9867	0.9347
	293	0.8332	0.844	0.9659	0.9747
	333	0.8192	0.8292	0.9505	0.9825

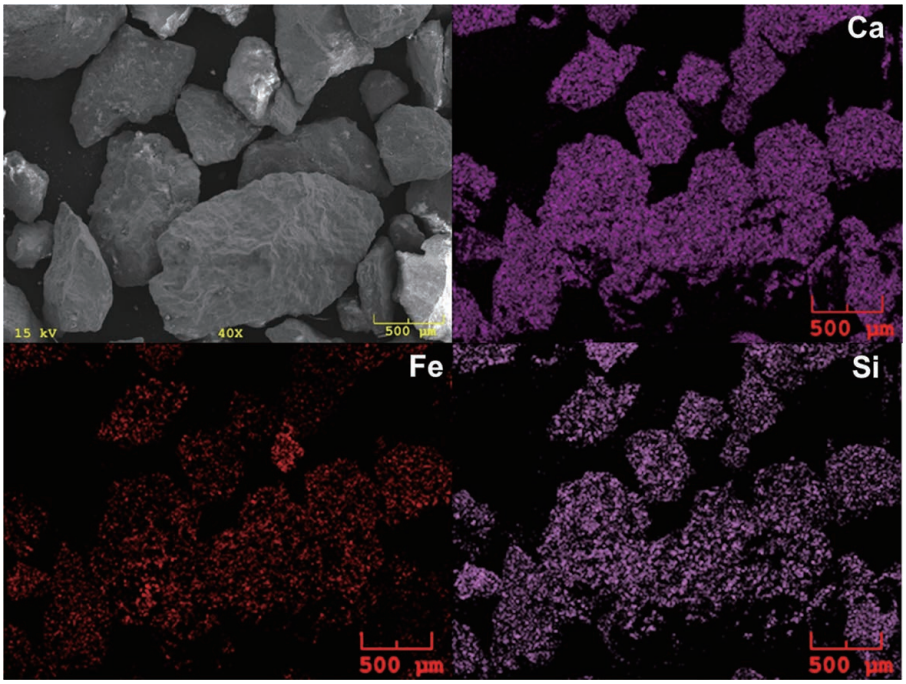

Fig. 9. SEM image and element mapping image of untreated sample.

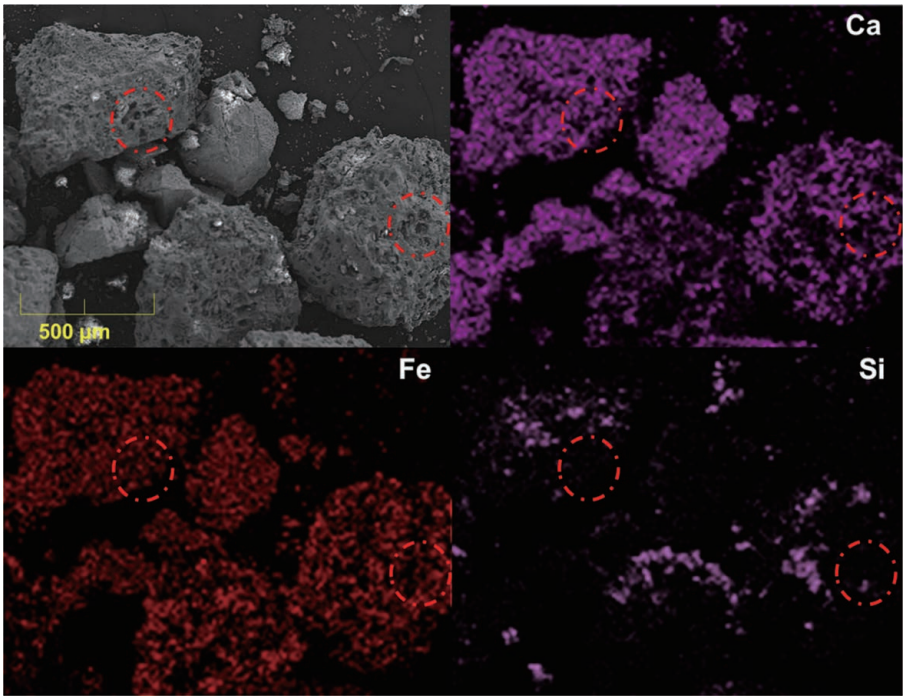

Fig. 10. SEM image and element mapping image of residue after leaching (acetic acid solution 0.28 mol/L, 293 K, 100 rpm).

ing process with stirring was linearized by logarithmic rate law. Therefore, it is presumed that some kind of coating was formed on the surface of residue during acetic acid leaching. For this reason, we observed the surface of residue after acetic acid leaching and untreated sample by using SEM-EDX (Hitachi High-Tech, S-3500H). **Figures 9** and **10** show the SEM images and element mapping images of Ca, Fe and Si; the residue in Fig. 10 is the sample after leaching in 0.28 mol/L acetic acid solution at the temperature of 293 K with stirring speed of 100 rpm.

Figure 9 indicates that the surface of untreated slag is relatively smooth and Ca of untreated sample surface is probably included mainly in Ca silicate phase due to the similar distribution of Ca and Si.

On the other hand, the residue after acetic acid leaching is porous material whose pores are blocked as shown in the area surrounded by red dashed borders of Fig. 10. Since it was reported that Ca phosphate phases such as dicalcium phosphate dihydrate, $CaHPO_4 \cdot 2H_2O$, and hydroxyapatite, $Ca_{10}(PO_4)_3(OH)_2$, could form in the steelmaking slag leachate,[33,34] the pores of slag particles might be blocked by these products during the leaching process. From the results of the Ca leaching process fitted well with logarithmic rate law and these SEM images, it is revealed that the mass transfer in the products blocking the pore surface of slag particles is very likely to be the rate-controlling step of Ca leaching.

Although Ca of untreated sample coexisted with Si as shown in Fig. 9, the element mapping images in Fig. 10 show that Ca of the residue after acetic acid leaching coexisted with Fe. Therefore, it is assumed that the Ca silicate phase of untreated slag dissolves due to acetic acid and then the poorly soluble phase in which Ca and Fe coexisted appears on the surface.

Moreover, the mineral phases after acetic acid leaching was investigated by XRD. **Figure 11** shows the XRD spectra of the residue after 300 min leaching in acetic acid solution. As can be seen in Fig. 11, the peak of larnite (Ca_2SiO_4) was detected although Si was hardly present on the surface of the residue after acetic acid leaching as shown in Fig. 10. Therefore, it is presumed that the Ca silicate phases on the surface of the slag particles dissolved but inside did not dissolve on the condition of this study.

3.6. Effect of Irradiation of Ultrasonic Wave

From the discussion in Section 3.4 and 3.5, it was found that the Ca leaching was very likely controlled by the mass transfer in the products blocking the pores of slag particles. Therefore, promoting the mass transfer in the products could enhance the rate of Ca leaching. For this reason, in this study, the effect of ultrasonic on the leaching of Ca and Fe from the steelmaking slag was investigated. In this experiment, ultrasonic wave was irradiated with ultrasonic cleaning bath provided by Emerson Japan, Ltd. The frequency is 42 kHz with a power of 70 W.

Ultrasonic can enhance the rate of mass transfer and reaction in homogeneous and heterogeneous systems. These effects are attributed to the implosive collapse of microbubbles (referred to as cavitation) which are formed during the negative pressure period of ultrasonic wave.[35] In fact, several studies have reported that ultrasonic irradiation could enhance the dissolution rate of oxides.[36–39]

Figures 12(a) and 12(b) show the Ca and Fe leaching curve, respectively. As can be seen from the results of Fig. 12(a), the leaching rate of Ca increases significantly with the ultrasonic irradiation. While the Ca leaching ratio reaches 56.6% at 300 min without ultrasonic irradiation, the leaching ratio reaches 57.3% just for 30 min leaching with ultrasonic irradiation; The leaching time at the Ca leaching ratio of about 57% could be shorten to one-tenth by promoting the mass transfer in the products blocking the pores of slag particles with ultrasonic irradiation. Said *et al.*[36] have investigated the effect of ultrasonic on the Ca leaching from steelmaking slag using ammonium chloride solution and reported that ultrasonic irradiation could enhance the Ca leaching rate effectively. Therefore, it is important to promote the mass transfer in the products blocking pores of slag particles for increasing the rate of Ca leaching.

On the other hand, the Fe leaching rate decreases by ultrasonic irradiation as shown in Fig. 12(b). Although the

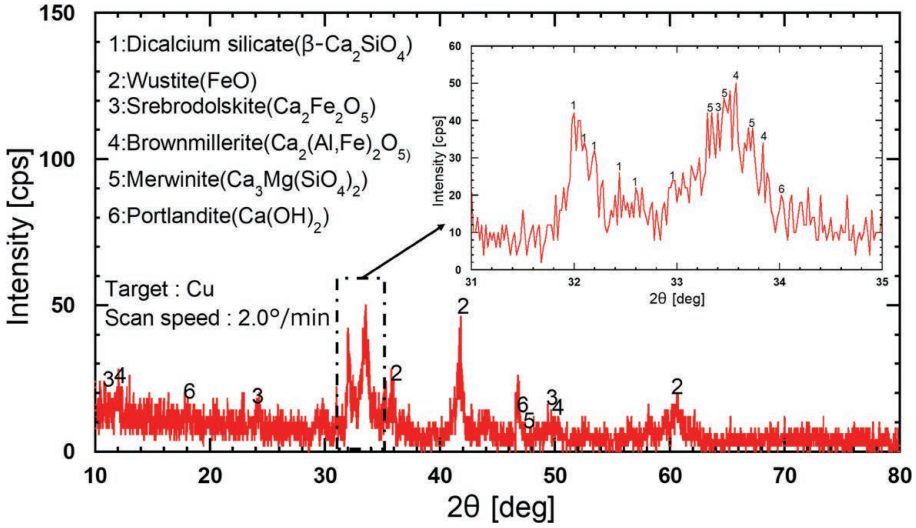

Fig. 11. XRD spectra of the residue after acetic acid leaching (acetic acid solution 0.28 mol/L, Solution temperature 293 K, stirring speed 100 rpm). The peak of larnite (1: β-Ca_2SiO_4) was detected although Si was hardly present on the surface of the residue after acetic acid leaching as shown in Fig. 10. (Online version in color.)

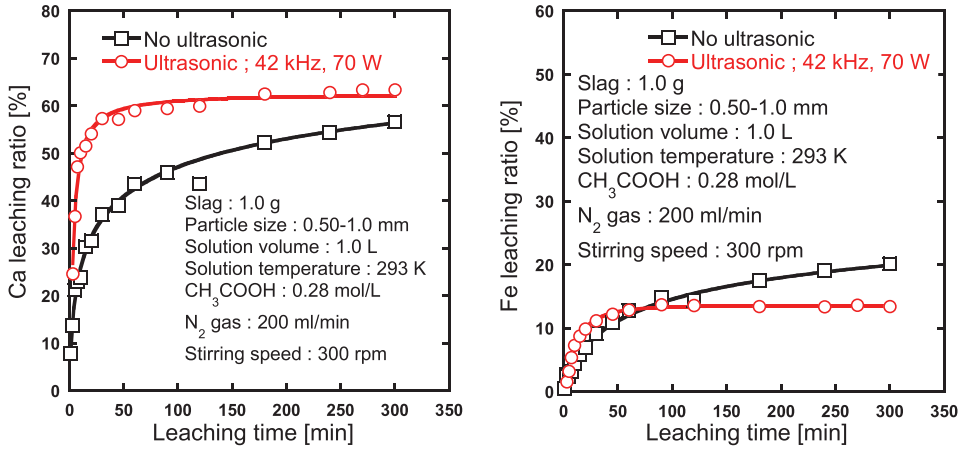

Fig. 12. Effect of ultrasonic for Ca leaching (a) and Fe leaching (b). (Online version in color.)

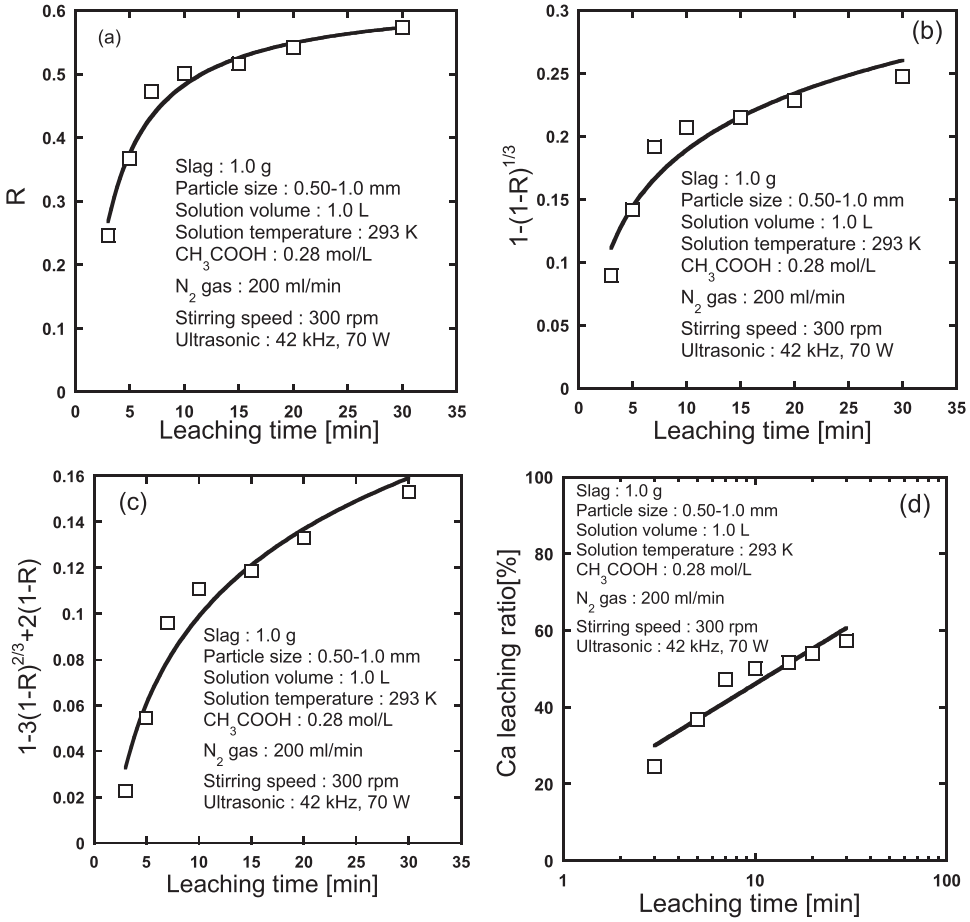

Fig. 13. Leaching kinetics model applied to Ca leaching with ultrasonic irradiation (Liquid film diffusion model (a), Surface chemical reaction model (b), Ash layer diffusion model (c), Logarithmic rate law (d)).

Fe leaching rate does not be affected by ultrasonic until 90 min, after that, the Fe leaching rate does not increase. The Fe leaching ratio without ultrasonic is 20.1% at 300 min, while the leaching ratio with ultrasonic is 13.4% at 300 min. Although this decrease of Fe leaching rate might be caused by the chemical effect due to ultrasonic, further investigations should be needed concerning this reason.

Furthermore, in this experiment, the rate of Ca and Fe leaching with ultrasonic irradiation were analyzed by leaching kinetics models. **Figures 13**(a)–13(d) and **14**(a)–14(d) show the plots of applying Eqs. (6)–(9), respectively, to the leaching behavior of Ca and Fe. In addition, the determination coefficients (R^2) in Figs. 13 and 14 are listed in **Table 4**. Note that the rate of Ca and Fe leaching were analyzed, respectively, in the range of 3 to 30 min and 3 to 90 min for discussing the stage from the beginning of leaching to equilibrium. As can be seen in Figs. 13 and 14, both the Ca and Fe leaching processes can be linearized by logarithmic rate law (Eq. (9)). Moreover, in Section 3.4, the Ca and Fe leaching processes without ultrasonic irradiation could be also fitted well by logarithmic rate law. Therefore, it was found that the rate-controlling step of the Ca leaching in the range of time discussed in this study was the mass transfer in the products blocking the pores of slag particles regard-

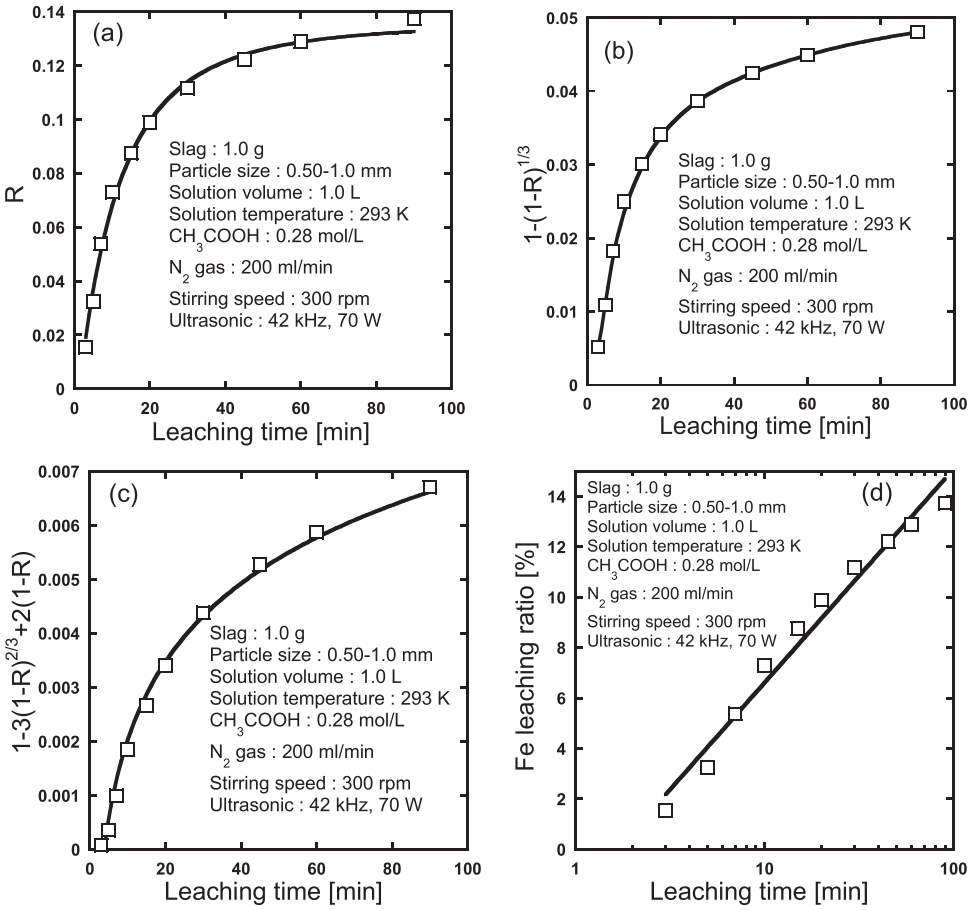

Fig. 14. Leaching kinetics model applied to Fe leaching with ultrasonic irradiation (Liquid film diffusion model (a), Surface chemical reaction model (b), Ash layer diffusion model (c), Logarithmic rate law (d)).

Table 4. The determination coefficients of various kinetics models with ultrasonic irradiation.

Element	Determination coefficients (R^2)			
	$R = kt$	$1-(1-R)^{1/3} = kt$	$1-3(1-R)^{2/3}+2(1-R) = kt$	$R = k \log t + C$
Ca	−2.597	0.6905	0.7719	0.8816
Fe	−0.079	−0.015	0.7698	0.9756

less of ultrasonic irradiation although the rate of Ca leaching could be increased considerably by ultrasonic irradiation.

4. Conclusion

In this study, the rate of Ca and Fe leaching from steelmaking slag in acetic acid were investigated and analyzed by shrinking core model (SCM) and logarithmic rate law for the purpose of understanding the Ca leaching. The results are listed as bellow:

(1) The Ca leaching rate increased as the acetic acid concentration increased. The Ca leaching ratio at the leaching time of 300 min was 7.2% without acetic acid, whereas the leaching ratio reached 56.6% at the concentration of 0.28 mol/L.

(2) Although the Ca and Fe leaching rate increased significantly up to 100 rpm, the leaching rate increased only slightly in the range of 100 to 300 rpm. The Ca leaching with stirring did not fit with the SCM but fitted well with logarithmic rate law in the range of 3 to 300 min. The Fe leaching also fitted well with logarithmic rate law except for the conditions without stirring. This result shows the possibility that some kind of coating was formed on the surface of slag particles during acetic acid leaching.

(3) The Ca leaching was hardly dependent on the solution temperature and could be linearized by logarithmic rate law in the range of 281–333 K. On the other hand, the Fe leaching rate was almost the same at 293 K and 333 K and followed logarithmic rate law. However, the Fe leaching rate at 281 K was lower than 293 K and 333 K and followed ash layer diffusion model.

(4) The SEM images of the residue after acetic acid leaching and untreated slag sample show that the surface of untreated slag was relatively smooth, whereas the slag particles after leaching were porous materials and the pores were blocked. From the results of kinetics analysis and SEM images, it was found that the Ca leaching in acetic acid from steelmaking slag was very likely controlled by the mass transfer in the products blocking pore surface of slag particles.

(5) The rate of Ca leaching could increase remarkably by promoting the mass transfer in the products blocking the

pore surface of slag particles. The Ca leaching ratio reached 57.3% just for 30 min with ultrasonic irradiation although the Ca leaching ratio reached 56.6% for 300 min leaching with mechanical stirring. Moreover, it was found that the Ca leaching could be linearized by logarithmic rate law as well as the Ca leaching without ultrasonic irradiation.

Acknowledgements

Parts of this work have been supported by The Iron and Steel Institute of Japan (Research Group of CCU for Iron and Steel Making).

REFERENCES

1) W. J. J. Huijgen, G. J. Witkamp and R. N. J. Comans: *Environ. Sci. Technol.*, **39** (2005), 9676. https://doi.org/10.1021/es050795f
2) R. Zevenhoven, S. Teir and S. Eloneva: *Energy*, **33** (2008), 362. https://doi.org/10.1016/j.energy.2007.11.005
3) E. R. Bobicki, Q. Liu, Z. Xu and H. Zeng: *Prog. Energy Combust. Sci.*, **38** (2012), 302. https://doi.org/10.1016/j.pecs.2011.11.002
4) S. Teir, S. Eloneva and R. Zevenhoven: *Energy Convers. Manag.*, **46** (2005), 2954. https://doi.org/10.1016/j.enconman.2005.02.009
5) G. Montes-Hernandez, R. Pérez-López, F. Renard, J. M. Nieto and L. Charlet: *J. Hazard. Mater.*, **161** (2009), 1347. https://doi.org/10.1016/j.jhazmat.2008.04.104
6) R. R. Tamilselvi Dananjayan, P. Kandasamy and R. Andimuthu: *J. Clean. Prod.*, **112** (2016), 4173. https://doi.org/10.1016/j.jclepro.2015.05.145
7) D. N. Huntzinger, J. S. Gierke, S. K. Kawatra, T. C. Eisele and L. L. Sutter: *Environ. Sci. Technol.*, **43** (2009), 1986. https://doi.org/10.1021/es802910z
8) S. N. Lekakh, C. H. Rawlins, D. G. C. Robertson, V. L. Richards and K. D. Peaslee: *Metall. Mater. Trans. B*, **39** (2008), 125. https://doi.org/10.1007/s11663-007-9112-8
9) N. L. Ukwattage, P. G. Ranjith and X. Li: *Measurement*, **97** (2017), 15. https://doi.org/10.1016/j.measurement.2016.10.057
10) M. Tu, H. Zhao, Z. Lei, L. Wang, D. Chen, H. Yu and T. Qi: *ISIJ Int.*, **55** (2015), 2509. https://doi.org/10.2355/isijinternational.ISIJINT-2015-142
11) Nippon Slag Association: Production and Uses of Steel Slag in Japan, https://www.slg.jp/pdf/Steel%20Slag%202017FY%20rev.pdf, (accessed 2020-10-28).
12) S. Y. Pan, R. Adhikari, Y. H. Chen, P. Li and P. C. Chiang: *J. Clean. Prod.*, **137** (2016), 617. https://doi.org/10.1016/j.jclepro.2016.07.112
13) Ministry of Environment, Government of Japan: On Greenhouse Gas Emissions (Confirmed Values) in 2018 (Heisei 30), (April, 2020), https://www.env.go.jp/earth/ondanka/ghg-mrv/emissions/results/material/yoin_2018_1.pdf, (accessed 2020-10-28) (in Japanese).
14) Ministry of Environment, Government of Japan: Energy-derived CO_2 in the Industrial Sector, (April, 2020), https://www.env.go.jp/earth/ondanka/ghg-mrv/emissions/results/material/yoin_2018_2_3.pdf, (accessed 2020-10-28) (in Japanese).
15) X. Zhang, H. Matsuura and F. Tsukihashi: *ISIJ Int.*, **52** (2012), 928. https://doi.org/10.2355/isijinternational.52.928
16) Z. Zhu, X. Gao, S. Ueda and S. Y. Kitamura: *ISIJ Int.*, **59** (2019), 1908. https://doi.org/10.2355/isijinternational.ISIJINT-2019-049
17) S. Yokoyama, A. Suzuki, H. B. M. N. Nik, H. Kanematsu, A. Ogawa, T. Takahashi, M. Izaki and M. Umemoto: *ISIJ Int.*, **50** (2010), 630. https://doi.org/10.2355/isijinternational.50.630
18) Y. Kashiwaya, S. Tauchi, T. Nomura and T. Akiyama: *ISIJ Int.*, **60** (2020), 2859. https://doi.org/10.2355/isijinternational.ISIJINT-2020-265
19) T. Iwama, C. M. Du, X. Gao, S. J. Kim, S. Ueda and S. Y. Kitamura: *ISIJ Int.*, **58** (2018), 1351. https://doi.org/10.2355/isijinternational.ISIJINT-2017-658
20) M. Numata, N. Maruoka, S. J. Kim and S. Y. Kitamura: *ISIJ Int.*, **54** (2014), 1983. https://doi.org/10.2355/isijinternational.54.1983
21) S. Teir, S. Eloneva, C. J. Fogelholm and R. Zevenhoven: *Energy*, **32** (2007), 528. https://doi.org/10.1016/j.energy.2006.06.023
22) S. Eloneva, S. Teir, J. Salminen, C. J. Fogelholm and R. Zevenhoven: *Ind. Eng. Chem. Res.*, **47** (2008), 7104. https://doi.org/10.1021/ie8004034
23) H. P. Mattila, I. Grigaliūnaitė and R. Zevenhoven: *Chem. Eng. J.*, **192** (2012), 77. https://doi.org/10.1016/j.cej.2012.03.068
24) A. Said, H. P. Mattila, M. Järvinen and R. Zevenhoven: *Appl. Energy*, **112** (2013), 765. https://doi.org/10.1016/j.apenergy.2012.12.042
25) C. Hall, D. J. Large, B. Adderley and H. M. West: *Miner. Eng.*, **65** (2014), 156. https://doi.org/10.1016/j.mineng.2014.06.002
26) R. Baciocchi, G. Costa, M. Di Gianfilippo, A. Polettini, R. Pomi and A. Stramazzo: *J. Hazard. Mater.*, **283** (2015), 302. https://doi.org/10.1016/j.jhazmat.2014.09.016
27) E. E. Chang, S. Y. Pan, Y. H. Chen, C. S. Tan and P. C. Chiang: *J. Hazard. Mater.*, **227**–**228** (2012), 97. https://doi.org/10.1016/j.jhazmat.2012.05.021
28) F. Habashi: Principles of Extractive Metallurgy Vol. 1, General Principles, Gordon and Breach, New York, (1970), 141.
29) O. Levenspiel: Chemical Reaction Engineering, 3rd ed., John Wiley & Sons, Hoboken, NJ, (1999), 567.
30) S. Gopinath and A. Mehra: *Chem. Eng. Res. Des.*, **115** (2016), 173. https://doi.org/10.1016/j.cherd.2016.09.010
31) R. C. Hubli, J. Mittra and A. K. Suri: *Hydrometallurgy*, **44** (1997), 125. https://doi.org/10.1016/S0304-386X(96)00036-9
32) A. Yazawa and M. Eguchi: Shissikiseiren-to-Haisuisyori (Hydrometallurgy and Wastewater Treatment), Kyoritsu Shuppan Co., Ltd., Tokyo, (1975), 55 (in Japanese).
33) C. M. Du, X. Gao, S. Ueda and S. Y. Kitamura: *ISIJ Int.*, **58** (2018), 833. https://doi.org/10.2355/isijinternational.ISIJINT-2017-454
34) T. Teratoko, N. Maruoka, H. Shibata and S. Y. Kitamura: *High Temp. Mater. Process.*, **31** (2012), 329. https://doi.org/10.1515/htmp-2012-0032
35) L. C. Hagenson and L. K. Doraiswamy: *Chem. Eng. Sci.*, **53** (1998), 131. https://doi.org/10.1016/S0009-2509(97)00193-0
36) A. Said, O. Mattila, S. Eloneva and M. Järvinen: *Chem. Eng. Process.*, **89** (2015), 1. https://doi.org/10.1016/j.cep.2014.12.008
37) B. Avvaru, S. B. Roy, S. Chowdhury, K. N. Hareendran and A. B. Pandit: *Ind. Eng. Chem. Res.*, **45** (2006), 7639. https://doi.org/10.1021/ie060599x
38) J. Ma, Y. Zhang, Y. Qin, Z. Wu, T. Wang and C. Wang: *Ultrason. Sonochem.*, **35** (2017), 304. https://doi.org/10.1016/j.ultsonch.2016.10.006
39) J. A. Barrera-Godinez, T. J. O'Keefe and J. L. Watson: *Miner. Eng.*, **5** (1992), 1365. https://doi.org/10.1016/0892-6875(92)90172-6